



Fuel constraints, not fire weather conditions, limit fire behavior in reburned boreal forests

Katherine Hayes^{a,b,*}, Chad M. Hoffman^c, Rodman Linn^d, Justin Ziegler^{c,e}, Brian Buma^{a,f}

^a Department of Integrative and Systems Biology, University of Colorado Denver, Campus Box 171 PO. Box 173364 Denver, CO 80217-3364, USA

^b Present: Cary Institute of Ecosystem Studies, 2801 Sharon Turnpike, Millbrook NY 12545, USA

^c Department of Forest and Rangeland Stewardship, Colorado State University, 1401 Campus Delivery Fort Collins, CO 80523-1401, USA

^d Los Alamos National Laboratory, P.O. Box 1663 Los Alamos, NM 87545, USA

^e Present: Aster Global Environmental Solutions, 3800 Clermont St. NW North Lawrence, OH 44666, USA

^f Present: Environmental Defense Fund, 2060 Broadway Suite 300 Boulder, CO 80302, USA

ARTICLE INFO

Keywords:

Fire
Boreal forests
Fire behavior
Self-Regulation
Fuel

ABSTRACT

Fire frequency in boreal forests has increased via longer burning seasons, drier conditions, and higher temperatures. However, fires have historically self-regulated via fuel limitations, mediating the effects of changes in climate and fire weather. Early post-fire boreal forests (10–15 years postfire) are often dominated by mixed conifer-broadleaf or broadleaf regeneration, considered less flammable due to the higher foliar moisture of broadleaf trees and shrubs compared to their more intact conifer counterparts. However, the strength of self-regulation in the context of changing fire weather and climate combined with the emergence of novel broadleaf forest communities and structures remains unclear. We quantified fuel composition, abundance, and structure in burned and reburned forests in Interior Alaska and used a physics-based fire behavior model (the Wildland-Urban Interface Fire Dynamics Simulator) to simulate how these unique patterns of fuel influence potential rates and sustainability of fire spread. In once-burned forests dominated by mixed conifer-broadleaf regeneration, extreme fire weather conditions allowed for sustained fire spread, suggesting that intense fire conditions can enable reburning, even 10 to 15 years following a previous high-severity fire. However, fire spread was not sustained in thrice-burned regenerating broadleaf forests, where regeneration was often dense but more clumped, and thus less connected, separated by patches of bare soil. Crown fire traveled an average of 50 meters into thrice-burned forests before dying out, even under extreme fire weather conditions. This work suggests that fire spread may be possible in once-burned regenerating forests under extreme fire weather conditions but may be more limited in less connected and less fuel abundant thrice-burned regenerating forests, at least within the 10–15-year window post-fire.

1. Introduction

Reburning is increasing in Interior Alaska due to warming temperatures, longer fire seasons (Lund et al., 2023), increased lightning (Veraverbeke et al., 2017) and drier conditions (Buma et al., 2022), threatening carbon storage (Balshi et al., 2009; Eckdahl et al., 2022) and complicating fire management efforts (Whitman et al., 2024). Historically, fires were infrequent (Hoecker and Higuera, 2019) and high-severity (producing complete canopy mortality), enforcing a ‘legacy lock’ on forest composition that allowed conifers, such as black spruce (*Picea mariana*), to dominate (Johnstone et al., 2010). Reburns in short intervals (defined as two fires in an interval of 50 years or less in

the boreal) and continued reburning (three or more fires in an interval of 150 years or less) drive stand-level transitions from conifer-dominated forests to broadleaf shrublands and grasslands (Hayes and Buma, 2021; Johnstone and Chapin, 2006). Broadleaf boreal forests have historically been less capable of igniting and carrying fire spread (Barrett et al., 2016) due to higher foliage moisture (Kelly et al., 2013) of dominant species like birch (*Betula neolaskana*) and aspen (*Populus tremuloides*), to such an extent that fire managers frequently rely on broadleaf forests as fire breaks (Whitman et al. 2024). Based on the higher foliar moisture of broadleaf individuals, several have hypothesized that an increased presence of broadleaf species across boreal forests could enable negative feedbacks to future fire (Brubaker et al.,

* Corresponding author.

E-mail address: hayesk@caryinstitute.org (K. Hayes).

<https://doi.org/10.1016/j.agrformet.2024.110216>

Received 7 September 2023; Received in revised form 16 August 2024; Accepted 3 September 2024

Available online 11 September 2024

0168-1923/© 2024 The Authors. Published by Elsevier B.V. This is an open access article under the CC BY license (<http://creativecommons.org/licenses/by/4.0/>).

2009), i.e., ‘self-regulation’ (Hart et al., 2019; Parks et al., 2015).

However, the strength, reliability, and potential duration of boreal self-regulation remains unclear, given two factors: one, ongoing reburning may shift forest community composition outside historic norms (Hayes and Buma, 2021) and two, extreme fire weather conditions may overwhelm foliar moisture constraints. To better evaluate the potential strength of broadleaf self-regulation in boreal forests under warming conditions, we need a stronger understanding of potential fire behavior in emerging broadleaf regeneration.

At a stand level, given adequate fire weather conditions, fire behavior is determined by the availability and arrangement of fuels. Both fuel abundance and arrangement are driven by forest structure and composition (Atchley et al., 2021; Parsons et al., 2017). In boreal Interior Alaska, forest composition (and therefore structure) has been remarkably stable for millennia under an infrequent, high severity fire regime (Kelly et al., 2013), which promoted black spruce dominance across the region. Broadleaf communities were present (Higuera et al., 2008; Kelly et al., 2013), but limited spatially, and predominantly birch (*Betula neolaskana*). However, paleoecological community types, which display self-regulation of fire across millennial time scales, are not analogous to modern emerging communities in Alaska: recent studies have found aspen (*Populus tremuloides*), alder (*Alnus crispa*), and willow (*Salix* spp.) in dominant quantities after reburning (Hayes and Buma, 2021; Johnstone et al., 2020). Shifts in forest composition are associated with corresponding shifts in forest structure: in forests that reburn, increased presence of species like aspen and willow lead to more open and more clumped spatial distribution of trees with each additional fire (Hayes and Buma, 2021). Tree density and distribution play an important role in fire behavior (Eckdahl et al., 2022; Hély et al., 2000): more open forest structure can alter wind flow, leading to shifts in ignitability and rate of spread (Pimont et al., 2011; Ryan, 2002). In addition, broadleaf species are faster-growing, outpacing black spruce regeneration (Mack et al., 2021) which could lead to greater fuel abundance. Currently, we lack modern empirical data on the spatial distribution and abundance of fuels in emerging broadleaf forests, limiting our ability to make informed hypotheses about potential fire behavior.

In addition, fire weather conditions are departing from historic or paleoecological norms in Alaska (Lund et al., 2023). The number of “extreme” fire seasons has increased in Alaska (“extreme” here referring to burned area, Turquetly et al., 2007), driven by increasingly warm and dry summers (Balshi et al., 2009; Lund et al., 2023). In the two extreme fire seasons of 2004 and 2005 (6.6 million acres burned in 2004, nearly 35 times the median annual area burned, Veraverbeke et al., 2015), spruce and broadleaf forests burned at similar frequencies (Chapin et al., 2010), suggesting foliar moisture constraints could be overridden. In addition, studies of the spatial distribution of contemporary reburning across Alaska found the effects of self-regulation are strongest within the first decade after fire but begin to decay within 10 to 20 years (Buma et al., 2022). Understanding the future characteristics of boreal fire regimes requires evaluating the combined role of shifts in community type, forest structure, and fire weather conditions and their potential cumulative impact on future fire behavior. The combined impact of novel community types, more open stand structures, and extreme climate-driven fire weather may enable fire to overcome previous self-regulation thresholds (Baltzer et al., 2021; Whitman et al., 2024, 2019).

One challenge in understanding potential future fire behavior is the intrinsic novelty of emerging forest types: many of our tools for understanding and predicting fire behavior depend on norms and relationships determined by historic observations (i.e., standardized indices of fuel types, Stocks et al., 1989). Emerging forest types with structures and compositions that differ from historic norms require models that can incorporate novel fuel characteristics and transitions between fuel types. Physics-based wildland fire behavior modeling, a type of deterministic model that attempt to include all known relevant factors influencing fire behavior, can be used to explore potential fire behavior in systems with

novel fuel characteristics (Hoffman et al., 2018). Here, we use the Wildland-Urban Interface Fire Dynamics Simulator (WFDS, version 9977), a physics-based fire behavior model that represents fuel composition and structure in three dimensions, accounting for bulk density, surface area to volume ratio, heat of combustion, and fuel moisture. WFDS has been used to explore hypothetical fire behavior in novel or complex fuel structures in other systems (Mell et al., 2010), including wildland fire in Wildland-Urban-Interfaces (Mell et al., 2011), bark beetle-infested forests (Hoffman et al., 2012, 2013), transitions between homogenous conifer forests and mixed conifer-broadleaf forests (Ziegler et al., 2021), and fuel hazard reduction and restoration treatments (Ritter et al., 2022; Ziegler et al., 2020).

The lack of relevant information on emerging broadleaf forests and their relationship with fire provides an ideal and timely opportunity to apply a physics-based model to questions related to fire behavior and fire self-regulation, topics of considerable importance for future boreal forest stability. Our objective was to evaluate how fuel composition, fuel density, and distribution change with increasing short-interval reburns to explore potential fire behavior across a gradient of fuel and weather conditions. We ask the following research questions:

1. How does fuel abundance and arrangement differ in burned, reburned, and thrice-burned forests?
2. Do differences in fuel abundance and arrangement enable differences in wind flow or windspeed during a potential fire event?
3. Given patterns of fuel abundance and arrangement in burned and reburned forests, can moderate or extreme fire weather conditions sustain crown fire spread?

To build on previous studies examining fuel characteristics after a single fire event (Boyd et al., 2023; Hammond et al., 2019), here we assess fuel abundance and arrangement in boreal forests that have experienced one to three short-interval sequential fires. We hypothesize that fuel abundance and connectivity will initially increase with additional fires via differences in arrangement but decrease after three short-interval fires as reburns continue to consume fuel. In addition, we hypothesize that shifts in fuel arrangement produced by shifts in forest regeneration will increase wind speed and change patterns of wind flow through reburned forests. Finally, we predict that extreme fire weather conditions (high winds and low fuel moisture) may enable sustained crown fire spread in reburned forests, potentially overwhelming fuel constraints (i.e., connectivity or abundance).

2. Materials and methods

2.1. Study area

To investigate how reburns alter fuel characteristics, we sampled spatial patterns of fuel abundance and arrangement at two locations in Interior Alaska. Each location experienced 1–3 fires within >30-year intervals. Across both locations, we randomly established 42 plots (each 20 by 20 meters) within burn perimeters, a minimum of 100 m apart and a minimum of 50 m from roads. We also established eight additional plots in the surrounding unburned forest as references for the assumed prefire conditions, for a total of 50 plots. Using tree cores, we checked burned and reburned plots for trees that may have survived individual fire events, and found none, indicating fires in both locations led to full canopy mortality.

2.2. Field sampling

To quantify fuel abundance, we measured dead downed woody debris, density and mass of live and dead standing fuels and the cover and abundance (mass and depth) of surface fuels. We measured dead down woody debris fuel loads (DWD, dead wood lying or standing below <45-degree angle) using two 28-m transects (Brown, 1974) radiating from the center of each of the 50 plots. We recorded the diameter, species, presence of charred material, and decay class of 1000-hour fuels

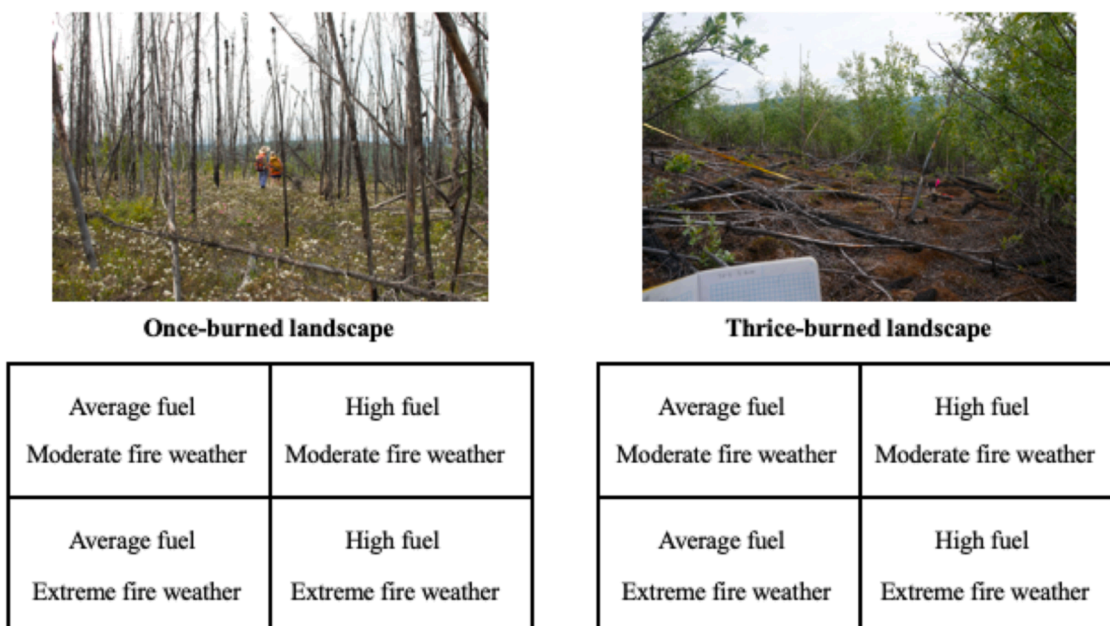


Fig. 1. Modeling Scenarios. Simulated landscapes were built using observed patterns of fuel abundance and arrangement from once-burned and thrice-burned forests (picture credit: Katherine Hayes), using mean values and 90th quartile values to represent an average fuel load and an extreme fuel load.

across the full transect and counted <3 cm fine debris across subsets (1-hr = 2 m, 10-hr = 5 m, 100-hr = 15 m). Total fuel loading (tons/ha) was calculated by converting DWD field data into estimates of mass per area (grams per meter) following [Brown \(1974\)](#). We measured mass of surface fuels (grass, litter, and shrubs) by harvesting randomly-located 1 × 1 m subplots (10 each, randomly located within the larger 20-by-20 m plots), drying vegetation for 48 h at 50 °C and then weighing. We measured surface fuel depth by recording height of the tallest vegetation (live and dead) connected continuously to the forest floor across 2-meter increments of the transect. We measured height and diameter at breast height (DBH 1.37 m) of standing live and dead trees in each plot in 200 m² randomly selected subsections. Where tree density precluded measuring the entire 200m², we measured 100m² subplots and scaled by area to produce estimates of tree density per m². We estimated total biomass of each species using a suite of local species-specific allometric equations (See Appendix: [Table S1](#) for specifics; [Binkley et al., 1984](#); [Bond-Lamberty et al., 2002](#)).

To capture differences in the arrangement of fuel, we calculated the spatial dispersion of trees using Eberhardt’s index, a metric of dispersion based on random point-to-nearest-organism-distance, for each species across each plot ([Hines and Hines, 1979](#)). We measured the distance to the nearest tree of each species present in the plot from a random point, selected by combinations of random distances from plot corners and replicated 10 times in each plot. We calculated Eberhardt’s index, as:

$$I_E = \left(\frac{s}{\bar{x}}\right)^2 + 1$$

where I_E = Eberhardt’s index of dispersion for point-to-organism distances, s = the observed standard deviation of distances, and \bar{x} = the mean of point-to-organism distances. The expected value of I_E in a random population is 1.27 – values below indicate a regular spatial pattern; values above indicate a clumped arrangement.

2.3. Fire modeling

To model wind flow and crown fire behavior based on the patterns of fuel abundance and arrangement we observed in burned and reburned forests, we used the Wildland-Urban Interface Fire Dynamics Simulator (WFDS), version 9977. WFDS version 9977 is based on Fire Dynamics

Simulator, developed by the National Institute of Standards and Technology (version 6, [McGrattan et al., 2012, 2024](#)). We chose WFDS over other modeling approaches for two reasons. First, it is a coupled fire-atmospheric model that provides spatial and temporal predictions of fire behavior based on a large eddy computational fluid dynamics model linked with models of thermal degradation, convective and radiative heat transfer, and gas-phase combustion. This coupled approach allows the model to capture emergent fire behavior associated with the interactions between fuel structures, wind flow, and fire. Second, WFDS represents heterogeneity in fuel load, moisture and physical characteristics in 3-dimensions providing the capacity to capture the complex fuel dynamics that occur in borders between dramatically different cover types ([Hoffman et al., 2018](#); [Mell et al., 2009](#)), such as those occurring between mature black spruce forests and regenerating broadleaf forests ([Boby et al., 2010](#); [Cahoon et al., 2022](#)). Further descriptions of the WFDS, including verification and validation, can be found in the following: ([Castle et al., 2013](#); [McGrattan et al., 2012](#); [Mell, 2007](#); [Mell et al., 2009](#); [Mueller et al., 2014](#); [Overholt et al., 2014](#); [Perez-Ramirez et al., 2017](#); [Ritter et al., 2020](#); [Sánchez-Monroy et al., 2019](#)). While smoldering combustion is an important characteristic of fire behavior in boreal forests, representing crown fire spread and smoldering simultaneously is not yet possible in WFDS or other fire behavior models, so we focus primarily on crown fire spread in this study.

Our simulation experiment was factorial ([Fig. 1](#)). We built model landscapes to compare once- and thrice-burned forests: while we measured fuel characteristics in twice-burned forests, we were constrained by computational resources and prioritized simulating landscapes with the greatest difference in fuel characteristics. We built two scenarios of fuel abundance and arrangement, referred to as “average fuel” and “high fuel”: average fuel scenarios were built using mean values of observed fuel abundance, and high fuel scenarios were built using the 90th quartile of observed values of fuel abundance. To test the role of fire weather conditions, we used 2 scenarios: moderate and extreme fire weather conditions. Moderate fire weather was simulated with an open (10-m above ground level) wind speed of 4 m s⁻¹, and conifer/hardwood foliar moisture contents of 97 % and 109 %, respectively. Extreme fire weather simulations had open (10-m above ground level) wind speeds of 8 m s⁻¹, and conifer/hardwood foliar moisture contents of 77 % and 89 %. We set surface fuel moisture at 10 % for both

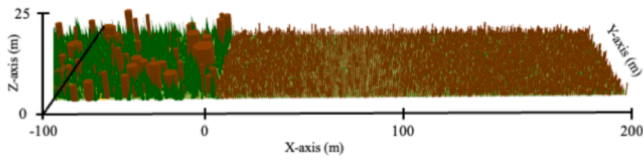


Fig. 2. Example of simulated Wildland-Urban Interface Fire Dynamics Simulator (WFDS) landscape. $X = 0$ represents the transition zone between unburned and burned landscapes. The Z-axis represents the height of the modeling domain, determined by the 90th quartile of the heights observed in the field. The Y-axis represents the width of the area tracked within the modeling domain and differs according to the model scenario: high-fuel scenarios produce too many trees to be tracked across the same space. Brown cones represent broadleaf species, green cylinders represent conifers.

Table 2

Characteristics of surface fuel and ground cover between once-burned and thriceburned forests.

Burn	Fuel Type	% Cover	Height (m)	Moisture (%)	Bulk Density (kg/m ³)	Load (kg/m ²)
1	Litter	13.9 %	0.04	20	2	0.02
	Litter, Herbs, Shrubs	86.2 %	0.243	38	3.64	0.0668
3	Litter	61.1 %	0.04	20	2	0.02
	Litter, herbs, shrubs	38.9 %	0.243	65	10.2	0.0238

Fuel loads across reburn history

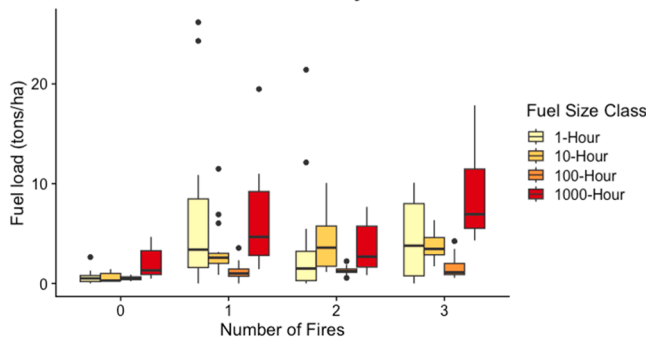


Fig. 3. Average mass fuel load by fuel size classes of dead down woody debris (Tons/Ha) across years since initial fire and between sites according to size classes (defined by the time scale at which moisture is lost). Dots represent outliers (defined as 1.5x the interquartile range less than the first quartile and greater than the third).

Table 1

Fuel abundance and density of trees (live/dead) within burns and scenarios. DBH is the average diameter of trees, measured in centimeters. Density is the number of trees per m². SD stands for standard deviation. Fuel load is measured in kilograms per square meter. Bulk density is measured in kilograms per cubic meter.

Burn	Fuel Scenario	Fuel Load (Kg/m ²)	Bulk Density (Kg/m ³)	Status	DBH (cm)	Density (trees/m ²)
1x	Mean	0.02	0.01	Live	0.7 (SD 0.5)	0.8
				Dead	3.2 (SD 2.7)	0.8
	High	0.03	0.017	Live	0.7 (SD 0.5)	1.4
				Dead	3.2 (SD 2.7)	1.4
3x	Mean	0.05	0.013	Live	1.2 (SD 0.9)	0.6
				Dead	0.9 (SD 0.8)	0.6
	High	0.11	0.029	Live	1.2 (SD 0.9)	1.4
				Dead	0.9 (SD 0.75)	1.4

the moderate and extreme fire weather scenarios: foliar moisture metrics were estimated from the National Fuel Moisture Database (United States Forest Service 2010) as the average (across 2011–2020) monthly minimum foliar moisture content.

To represent the average patterns of fuel abundance and arrangement found in once- and thrice-burned forests, we distributed the mean

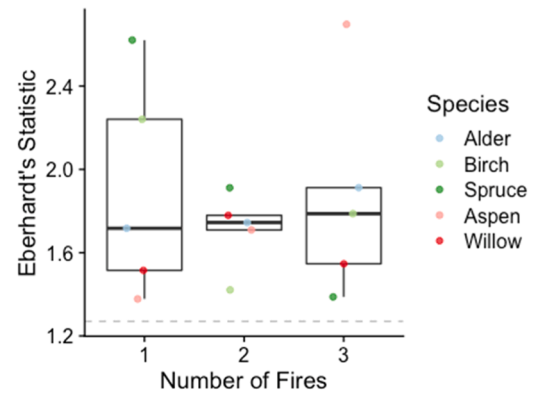


Fig. 4. Eberhardt's index (a metric of dispersion based on random point-to-nearest-organism distances) across reburn history. The expected value in a randomly-arranged population is 1.27; values below indicate a regular spatial pattern and values above indicate a clumped arrangement.

density of trees across our model domain and pulled from our distributions of composition, height, and DBH to assign each tree a species, live/dead status, height, and volume. To represent extreme fuel loads, we distributed the 90th quartile density of trees across the same 800 m × 300 m landscape, and pulled from the same distributions of composition, height, and DBH to assign tree characteristics (code available online: [10.5281/zenodo.10845722](https://doi.org/10.5281/zenodo.10845722)). In all scenarios, conifers were represented as cones, and broadleaf species were represented as cylinders. To capture the transition of fire from unburned to burned or reburned forests, and to “prime” crown fire spread, we started each modeled fire simulation with an ignition in unburned forest. We built our model of unburned forest based on measurements of fuel abundance and arrangement in our unburned reference plots (Fig. 2), following the approach described above.

The simulation domains were 560 m in the streamwise direction, 70 m in the spanwise direction, and 95 m tall. While domain size was consistent across simulations, we tracked different numbers of trees in average- vs high-fuel scenarios (the high number of trees in the high-fuel scenario produced computational restraints). Burned and reburned fuel landscapes began 360 m from the inlet of the domain at a location labelled $x = 0$ and extended to the outlet of the domain 200 m downwind of the transition at $x = 200$ m. Upwind unburned forest fuels spanned from $x = -360$ to $x = 0$ m. Inlets ($x = -360$ m) had wind entering, following a typical wind profile power law function:

$$U_z = U_r \left(\frac{z}{z_r} \right)^{1/7}$$

where U_r was either 4 m s⁻¹ or 8 m s⁻¹ depending on our specific simulation case and z_r was 10 m. Wind exited at $x = 200$ m. We ran each

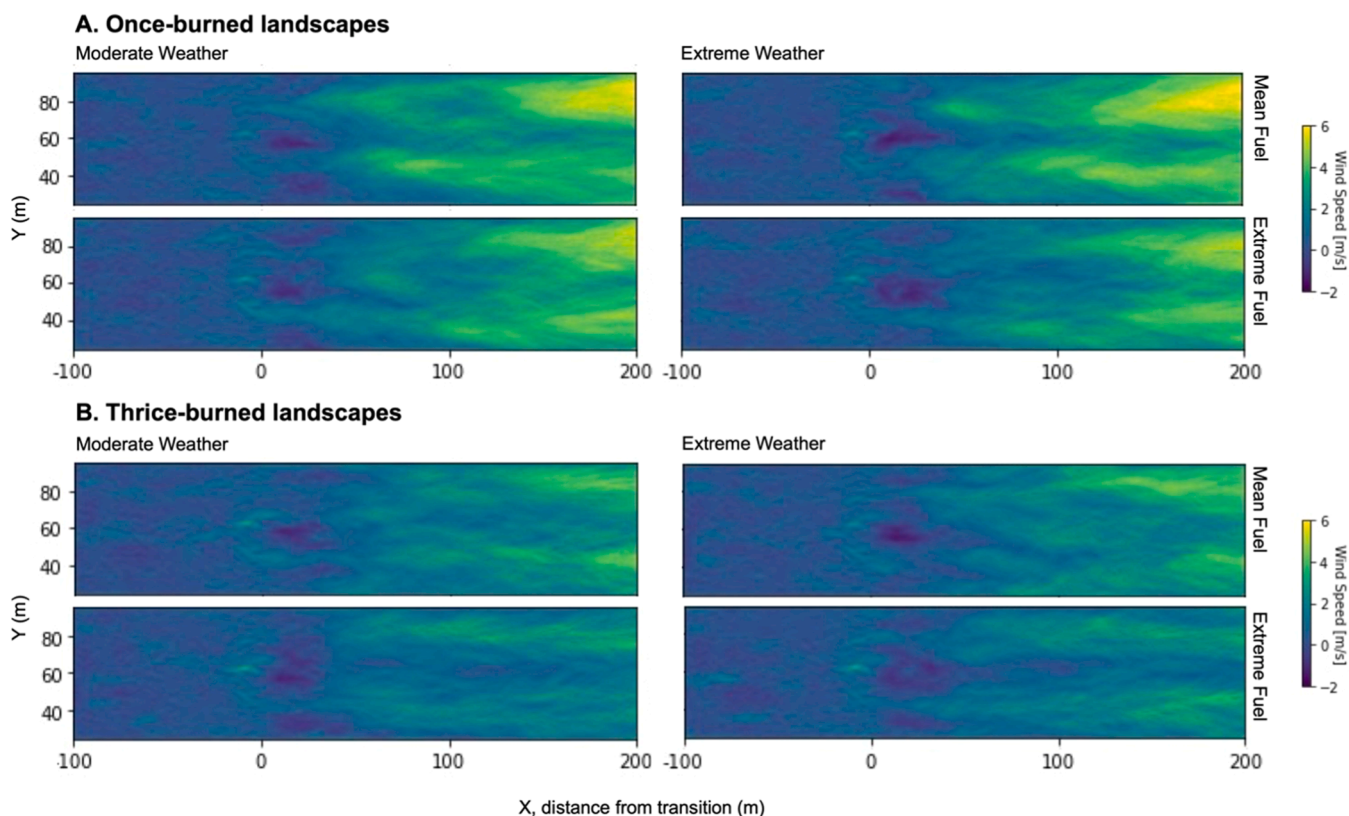


Fig. 5. Wind flow across scenario landscapes (in meters per seconds). $X = -100$ to 0 is the mature unburned simulated landscape, $X = 0$ is the start of the transition point, and $X = 0$ to 200 is the reburned simulated landscape. A) Wind flow across all scenarios of once-burned simulated landscapes. B) Wind flow across all scenarios of simulated thrice-burned landscapes.

simulation for 1000 seconds.

We represented surface fuel loads using the combined mean values of understory vegetation weight and seedling weight per square meter. We did not vary the bulk density and mass of surface fuels between the average and extreme fuel scenarios, but varied the ratio of litter to litter/herb/shrub. Based on observations of percent cover, we distributed two forms of surface fuels across each landscape: 1) a representative litter layer that included litter, lichen, fine fuels, and other organic materials, and 2) a litter, herb and shrub layer that included woody surface fuels (Fig. S2).

To explore how the characteristics of potential fire behavior differed across fuel/weather/burn scenarios, we tracked the wind velocity (2 m above ground level in m s^{-1}) (prior to fire ignition), time of arrival (s), rate of spread (m s^{-1}), and surface and canopy fuel consumption in each simulation. Rate of spread was calculated in m s^{-1} using loess smoothing of the time of arrival for each pixel from $X = 0$. Time of arrival represents the first time in seconds a loss of biomass is observed in each given pixel. These metrics are directly linked to fire behavior properties that direct the subsequent total area burned, fire severity, and fire management conditions. Fuel consumption results are presented in the Appendix. Because of the relatively low number of replications (due to processing time), and the deterministic nature of WFDS, we present the results qualitatively.

3. Results

3.1. How does fuel abundance and arrangement differ in burned, reburned, and thrice-burned forests?

3.1.1. Fuel abundance

Fuel abundance, as represented by the biomass held in downed woody debris, standing live and dead trees and surface fuels, was greater

in reburned forests than burned forests, but differed greatly across pools. The abundance of downed woody fuel in all size classes increased with reburning, but differed across specific reburn history and size classes. Fine fuels (1- and 10-hour fuels) were most abundant in the once- and twice-burned forests, increasing by an average factor of three after one fire, decreasing by a factor of 1.6 after two fires, and increasing by a factor of two after three fires. Large fuels (1000-hour fuels) followed a similar trend, increasing by a factor of 8 after one fire, declining after the second, and reaching a maximum average of 4.29 tons per ha after three fires. Medium fuel size classes (100-hours) increased after one fire but did not change meaningfully between reburning (Fig. 3).

The density and mass of standing fuels (live and dead trees) between once-burned and thrice-burned forests: once-burned forests contained greater numbers of dead trees, primarily spruce, killed in the first fire. Spruce had the highest DBH in the dataset and thus contained the greatest mass. Tree height was greatest in once-burned forests, again due to the increased presence of dead spruce in the landscape (species height distributions are presented in Appendix: Fig. S1). Trees were generally less dense in once-burned forests. In both the once- and thrice-burned scenarios, using the 90th quantile of tree density observations doubled the number of trees in the simulation, and roughly doubled the fuel load and density (Table 1).

3.1.2. Fuel arrangement

The arrangement of fuels differed between once- and thrice-burned forests. Surface fuels were less connected in thrice-burned forests than in once-burned forests (Fig. S2). Once-burned forests had greater surface fuel cover and fine fuel loads than thrice-burned forests (Table 2, Fig. S2).

Trees of all species displayed a non-random spatial distribution (Fig. 4). While Eberhardt's index for all species was above the 1.27 random pattern threshold, the spatial dispersion of species differed

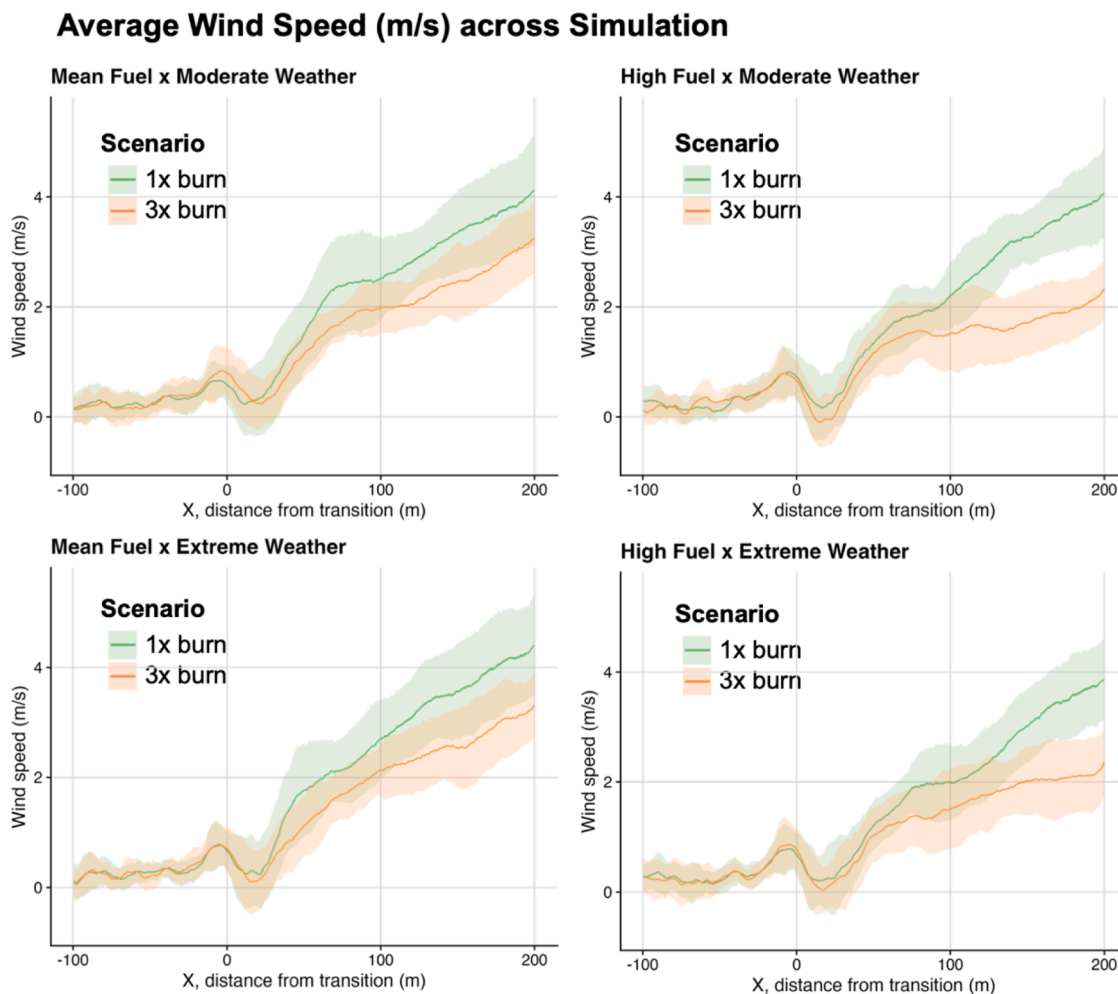


Fig. 6. Wind speed (in meters per second) averaged across the y-axis of model scenarios. Line represents average wind speed, band around line represents standard deviation.

between once-burned and thrice-burned forests. Variability among species was the greatest in the once- and thrice-burned forests. Aspen in particular show the greatest change across burn history, increasing from an index value of 1.37 to 1.71 to 2.69 after three fires, indicating a more clumped spatial pattern.

3.2. Do differences in fuel abundance and arrangement enable differences in wind flow or wind speed during a potential fire event?

3.2.1. Wind flow

Simulations showed a typical forest canopy flow upwind of the transition point ($x = 0$) consisting of a turbulent field with sweeps and jet formation acting as the primary mechanism for upward and downwards air movement. As the flow approaches the transition point, there was a reversal of the canopy flow direction associated with the detachment of the above canopy flow and void in pressure on the upwind edge of the unburned forest canopy. After 50–100 m, the flow above the canopy flow reattached (Fig. 5), resulting in a significant increase in wind speed (Fig. 6).

3.2.2. Wind speed

Wind speeds were slightly higher in mean fuel scenarios than in high fuel scenarios, regardless of the burn history. The primary difference between burn scenarios was the slightly faster wind speeds present towards the edge of the once-burned simulated landscape ($x = 100$ to 200, wind speeds reach 6 m s^{-1} , Fig. 6) compared to the thrice-burned

landscape (in the same region, wind speeds reach 4 m s^{-1} ; Fig. 6).

3.3. Given patterns of fuel abundance and arrangement in burned and reburned forests, can moderate or extreme fire weather conditions sustain crown fire spread?

Within each scenario, trends in the rate of spread of the fire initially followed trends in wind speed; as wind speed dropped after the transition point at $x = 0$ (Fig. 6), the rate of spread declined in all scenarios (Fig. 7). As wind speed began to pick back up with increasing distance from the transition point, rate of spread did as well. However, across all scenarios, the rate of spread and wind eventually diverged. While wind speed continued to increase with distance from the transition point in all scenarios, only the once-burned, mean fuel, and extreme fire weather scenarios continued to burn past 50–75 m beyond the transition point.

Out of the eight total scenarios, only one (once-burned, mean fuel, and extreme weather) experienced sustained crown fire spread across the majority of the domain. In all other scenarios, crown fire spread burned into the reburned landscape and halted within 50–75 m beyond the transition point $x = 0$. Both the once-burned and thrice-burned scenarios burned in WFDS, but crown fire behavior differed greatly between reburn histories. In both the once-burned and thrice-burned landscapes, bare patches of ground seemed to prevent crown fire spread, as demonstrated in both the high-fuel + extreme weather scenarios, in which the fire forked in two directions owing to the presence of a bare patch (Fig. 8A, Fig. 8B).

Rate of Spread (m/s) across Simulation

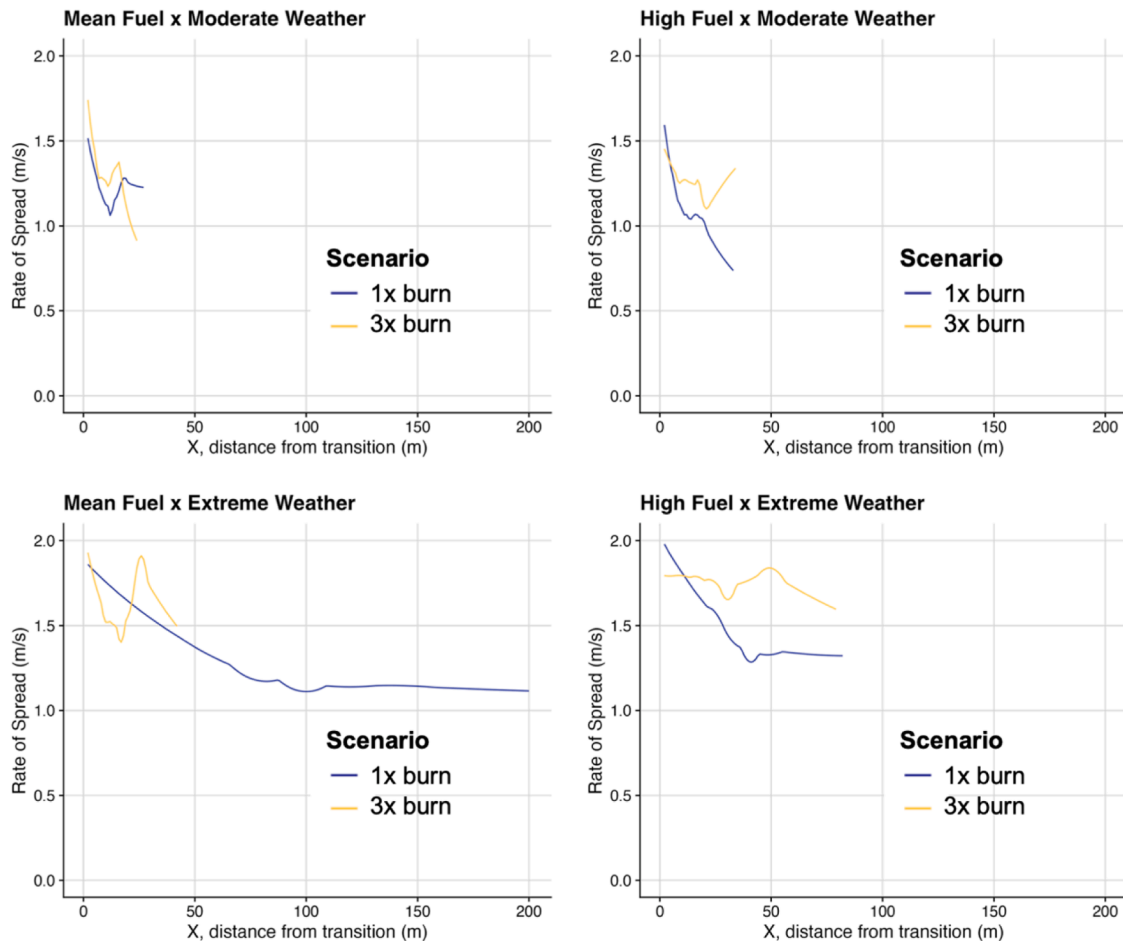


Fig. 7. Rate of fire spread, in meters per second, across 200 m of X beginning with the transition from simulated mature to reburned landscapes for each fuel/weather/burn scenario.

4. Discussion

Overall fuel abundance was greater in reburned stands compared to once-burned or unburned stands, and the largest differences between fire history were in fine and large fuel size classes. Connectivity of both surface and canopy fuels was lower in reburned landscapes; trees were more clumped and bare patches of ground were most abundant in thrice-burned landscapes.

Once-burned landscapes displayed a greater rate of spread than thrice-burned landscapes; fire spread was rarely sustained 50 m beyond the transition point in thrice-burned simulations, even under high fuel and extreme weather conditions. Under the conditions tested, this indicates fuel constraints may not be overcome by fire weather in thrice-burned landscapes. This finding is consistent with the results of other models applied in Interior Alaska: process-based models like the University of Virginia Forest Model Enhanced found that declines in fuel abundance led to lower fire severity and intensity in forests with greater presence of broadleaf species (Foster et al., 2022). One element that remains unclear is the relative importance of fuel abundance vs. fuel connectivity; untangling the roles of each individual fuel characteristic is critical to anticipating future fire behavior, but difficult under our current limited understanding of fire propagation (Hanan et al., 2022; Werth et al., 2011).

We observed limited crown fire spread into burned or reburned landscapes, indicating a what is sometimes referred to as a “transition zone” in fire behavior modeling. Transition zones and differences in

modeled fire behavior between two types of fuels (i.e., unburned vs. burned or structure vs. wildland) are observable in a variety of ecosystem types. WFDS simulations of red pine and other forest types in the western United States displayed transition zones from 6 m to 300 m (Ritter et al., 2022). Prior to this, transition zones between burned and unburned forests in the interior have not been simulated using a combustion model, but have been documented by fire managers across the state. We did not observe a consistent rate of spread in the majority of scenarios >75 m from the border between burned and unburned forest, implying fire spread is limited in continuous reburned landscapes.

Our modeling here makes several important simplifying assumptions around fire behavior in boreal forests. First, smoldering fires are a key element of boreal fires (Ryan, 2002). However, we observed shallow or non-existent soil organic layers in emerging broadleaf reburned forests (Hayes and Buma, 2021), which might imply smoldering may be limited in such forest types. While we do not expect these fuels to play a significant role in fire spread in broadleaf forests over the temporal scales simulated, they may be important on a larger scale. Very few fire behavior models can simulate smoldering and fire spread simultaneously at a scale relevant to both forms of combustion. Future work that examines the role of smoldering combustion in broadleaf forests or the transition between smoldering and spreading in boreal fuel types more generally would help fill this gap. Secondly, while WFDS is well validated for similar systems and fuel types, it remains unvalidated for boreal systems. Given that our work is explorative and not predictive, WFDS remains a powerful tool for exploring novel fuel characteristics,

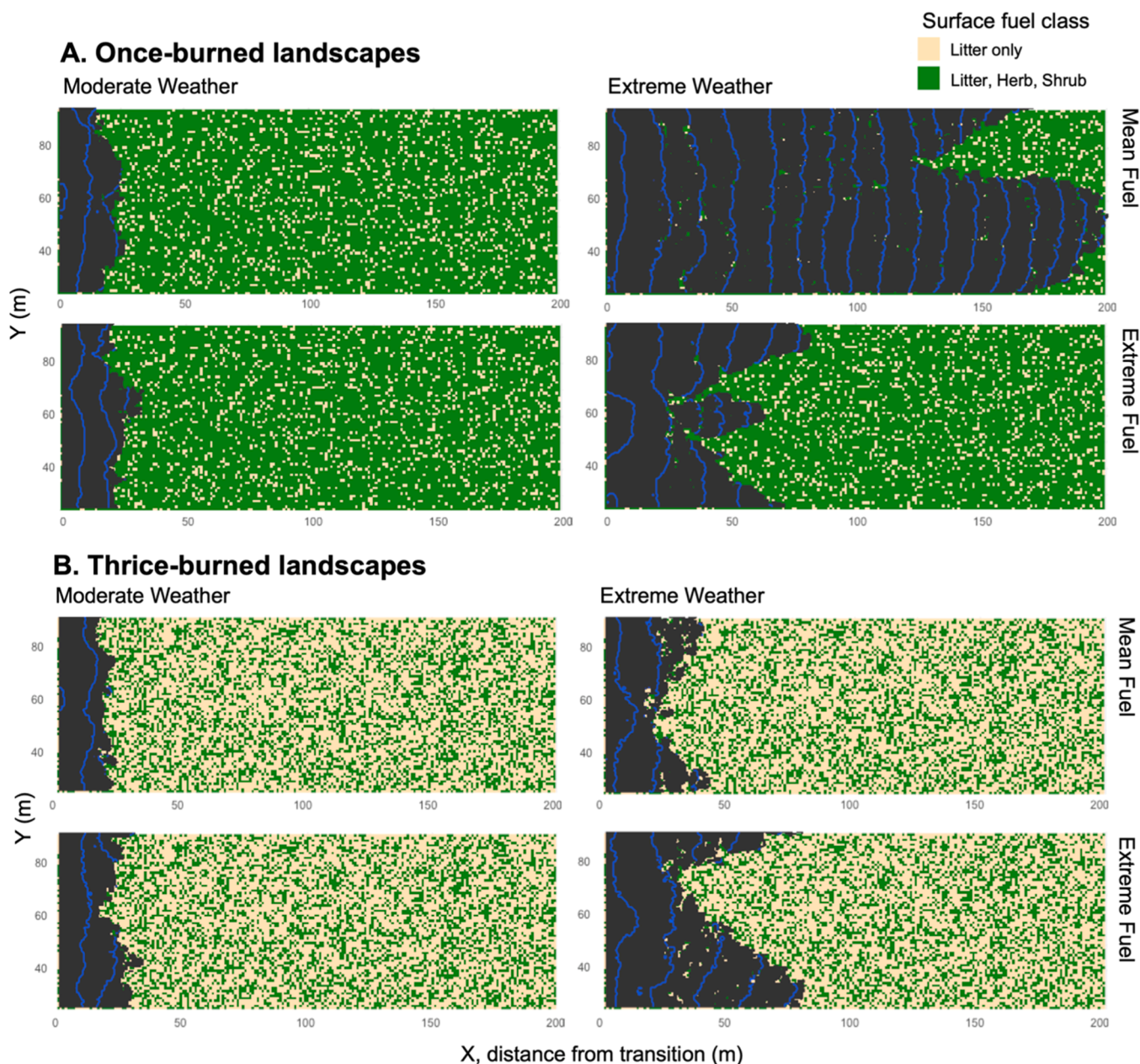


Fig. 8. Time of arrival of crown fire, measured as the first measurable loss of biomass within a given pixel, shown in two dimensions. $X = 0$ at the bottom left indicates the start of the burned fuels and the beginning of the transition between the mature and burned landscapes. Contours represent 10 second intervals. A) Once-burned landscape. B) Thrice-burned landscape.

but comparing WFDS modeled fire behavior with data from observed prescribed fire would help confirm the accuracy of this approach in boreal forests.

Self-regulation via the presence of higher moisture broadleaf species has been invoked as a landscape management solution to boreal warming (Astrup et al., 2018), based on paleoecological evidence of declining fire activity found alongside increases in the presence of birch pollen (Brubaker et al., 2009; Kelly et al., 2013). Our finding that simulated fire spread did not sustain in thrice-burned landscapes, even under extreme conditions, suggests that fuel constraints outweigh fire weather conditions, at least during the initial decades of post-fire regeneration. More information on the persistence of this self-regulation as stands age will be critical - our simulated reburned landscapes were based on the observed characteristics of 15-year-old regenerated forests. Current rates of reburning across Interior Alaska and beyond suggest that self-regulation persists across the first two

decades after fire (Buma et al., 2022; Whitman et al., 2024), which is consistent with our findings. Future work exploring the threshold of fuel abundance or connectivity that prevents fire spread in reburned forests will be critical to anticipating fire risk as stands continue to mature or as fire weather conditions change.

CRediT authorship contribution statement

Katherine Hayes: Conceptualization, Data curation, Formal analysis, Investigation, Methodology, Visualization, Writing – original draft, Writing – review & editing. **Chad M. Hoffman:** Conceptualization, Funding acquisition, Project administration, Resources, Software, Supervision, Writing – original draft, Writing – review & editing. **Rodman Linn:** Supervision, Writing – review & editing. **Justin Ziegler:** Methodology, Resources, Software, Writing – review & editing. **Brian Buma:** Conceptualization, Funding acquisition, Resources, Supervision,

Writing – review & editing.

Declaration of competing interest

The authors declare the following financial interests/personal relationships which may be considered as potential competing interests:

Brian Buma reports financial support was provided by National Science Foundation Division of Polar Programs. Katherine Hayes reports financial support was provided by Joint Fire Science Program.

Data availability

Data used in this research is available on zenodo ([10.5281/zenodo.10845722](https://doi.org/10.5281/zenodo.10845722)) and in a github repository (k8hayes/FireBehavior).

Acknowledgements

This study was funded by support from the NSF Office of Polar Programs (OPP:1903231 and OPP: 2215120) and a Graduate Innovation Award from the Joint Fire Science Program (ID 19–1-01–43). We are grateful to Vishnusai Kodicherla, Kyle Martini, Kristin Olson, Pauline Allen, and Teagan Furbish for their help in the field.

Supplementary materials

Supplementary material associated with this article can be found, in the online version, at [doi:10.1016/j.agrformet.2024.110216](https://doi.org/10.1016/j.agrformet.2024.110216).

References

- Astrup, R., Bernier, P.Y., Genet, H., Lutz, D.A., 2018. A sensible climate solution for the boreal forest. *Nat. Clim. Chang.*
- Atchley, A.L., Linn, R., Jonko, A., Hoffman, C., Hyman, J.D., Pimont, F., Sieg, C., Middleton, R.S., 2021. Effects of fuel spatial distribution on wildland fire behaviour. *Int. J. Wildland Fire* 30, 179.
- Balshi, M.S., McGuire, A.D., Duffy, P., Flannigan, M., Kicklighter, D.W., Melillo, J., 2009. Vulnerability of carbon storage in North American boreal forests to wildfires during the 21st century. *Glob. Change Biol.* 15, 1491–1510. <https://doi.org/10.1111/j.1365-2486.2009.01877.x>.
- Baltzer, J.L., Day, N.J., Walker, X.J., Greene, D., Mack, M.C., Alexander, H.D., Arseneault, D., Barnes, J., Bergeron, Y., Boucher, Y., Bourgeau-Chavez, L., Brown, C. D., Carrière, S., Howard, B.K., Gauthier, S., Parisien, M.-A., Reid, K.A., Rogers, B.M., Roland, C., Sirois, L., Stehn, S., Thompson, D.K., Turetsky, M.R., Veraverbeke, S., Whitman, E., Yang, J., Johnstone, J.F., 2021. Increasing fire and the decline of fire adapted black spruce in the boreal forest. *Proc. Natl. Acad. Sci.* 118, e2024872118. <https://doi.org/10.1073/pnas.2024872118>.
- Barrett, K., Loboda, T., McGuire, A.D., Genet, H., Hoy, E., Kasischke, E., 2016. Static and dynamic controls on fire activity at moderate spatial and temporal scales in the Alaskan boreal forest. *Ecosphere* 7, e01572. <https://doi.org/10.1002/ecs2.1572>.
- Binkley, D., Lousier, J.D., Cromack, K., 1984. Ecosystem effects of Sitka alder in a Douglas-fir plantation. *Forest Sci.* 30, 26–35.
- Boby, L.A., Schuur, E.A.G., Mack, M.C., Verbyla, D., Johnstone, J.F., 2010. Quantifying fire severity, carbon, and nitrogen emissions in Alaska's boreal forest. *Ecol. Appl.* 20, 1633–1647. <https://doi.org/10.1890/08-2295.1>.
- Bond-Lamberty, B., Wang, C., Gower, S.T., 2002. Aboveground and belowground biomass and sapwood area allometric equations for six boreal tree species of northern Manitoba 32, 10.
- Boyd, M.A., Walker, X.J., Barnes, J., Celis, G., Goetz, S.J., Johnstone, J.F., Link, N.T., Melvin, A.M., Saperstein, L., Schuur, E.A., 2023. Decadal impacts of wildfire fuel reduction treatments on ecosystem characteristics and fire behavior in Alaskan boreal forests. *For. Ecol. Manag.* 546, 121347.
- Brown, J.K., 1974. Handbook For Inventorying Downed Woody Material (No. 24). US Department of Agriculture, Forest Service, Intermountain Forest and Range Experiment Station.
- Brubaker, L.B., Higuera, P.E., Rupp, T.S., Olson, M.A., Anderson, P.M., Hu, F.S., 2009. Linking sediment-charcoal records and ecological modeling to understand causes of fire-regime change in boreal forests. *Ecology* 90, 1788–1801. <https://doi.org/10.1890/08-0797.1>.
- Buma, B., Hayes, K., Weiss, S., Lucash, M., 2022. Short-interval fires increasing in the Alaskan boreal forest as fire self-regulation decays across forest types. *Sci. Rep.* 12, 4901. <https://doi.org/10.1038/s41598-022-08912-8>.
- Cahoon, S.M.P., Sullivan, P.F., Gray, A.N., 2022. Interactions among wildfire, forest type and landscape position are key determinants of boreal forest carbon stocks. *J. Ecol.* 110, 2475–2492. <https://doi.org/10.1111/1365-2745.13963>.
- Castle, D., Mell, W.E., Miller, F.J., 2013. Examination of the wildland-urban interface fire dynamics simulator in modeling of laboratory-scale surface-to-crown fire transition. *Chapin, F.S., McGuire, A.D., Ruess, R.W., Hollingsworth, T.N., Mack, M.C., Johnstone, J. F., Kasischke, E.S., Euskirchen, E.S., Jones, J.B., Jorgenson, M.T., Kielland, K., Kofinas, G.P., Turetsky, M.R., Yarie, J., Lloyd, A.H., Taylor, D.L., 2010. Resilience of Alaska's boreal forest to climatic change. Can. J. For. Res., The Dynamics of Change in Alaska's Boreal Forests: Resilience and Vulnerability in Response to Climate Warming.* 40, 1360–1370. <https://doi.org/10.1139/X10-074>.
- Eckdahl, J.A., Kristensen, J.A., Metcalfe, D.B., 2022. Climatic variation drives loss and restructuring of carbon and nitrogen in boreal forest wildfire. *Biogeosciences* 19, 2487–2506. <https://doi.org/10.5194/bg-19-2487-2022>.
- Foster, A.C., Wang, J.A., Frost, G.V., Davidson, S.J., Hoy, E., Turner, K.W., Sonnentag, O., Epstein, H., Berner, L.T., Armstrong, A.H., 2022. Disturbances in North American boreal forest and Arctic tundra: impacts, interactions, and responses. *Environ. Res. Lett* 17, 113001.
- Hammond, D.H., Strand, E.K., Hudak, A.T., Newingham, B.A., 2019. Boreal forest vegetation and fuel conditions 12 years after the 2004 Taylor Complex fires in Alaska. *USA. Fire Ecol.* 15 (32) <https://doi.org/10.1186/s42408-019-0049-5>.
- Hanan, E.J., Kennedy, M.C., Ren, J., Johnson, M.C., Smith, A.M.S., 2022. Missing Climate Feedbacks in Fire Models: Limitations and Uncertainties in Fuel Loadings and the Role of Decomposition in Fine Fuel Accumulation. *J. Adv. Model. Earth Syst.* 14 <https://doi.org/10.1029/2021MS002818> e2021MS002818.
- Hart, S.J., Henkelman, J., McLoughlin, P.D., Nielsen, S.E., Truchon-Savard, A., Johnstone, J.F., 2019. Examining forest resilience to changing fire frequency in a fire-prone region of boreal forest. *Glob. Change Biol.* 25, 869–884. <https://doi.org/10.1111/gcb.14550>.
- Hayes, K., Buma, B., 2021. Effects of short-interval disturbances continue to accumulate, overwhelming variability in local resilience. *Ecosphere* 12. <https://doi.org/10.1002/ecs2.3379>.
- Hély, C., Bergeron, Y., Flannigan, M.D., 2000. Effects of Stand Composition on Fire Hazard in Mixed-Wood Canadian Boreal Forest. *J. Veg. Sci.* 11, 813–824. <https://doi.org/10.2307/3236551>.
- Higuera, P.E., Brubaker, L.B., Anderson, P.M., Brown, T.A., Kennedy, A.T., Hu, F.S., 2008. Frequent Fires in Ancient Shrub Tundra: Implications of Paleorecords for Arctic Environmental Change. *PLoS ONE* 3, e0001744. <https://doi.org/10.1371/journal.pone.0001744>.
- Hines, W.G.S., Hines, R.J.O., 1979. The Eberhardt statistic and the detection of nonrandomness of spatial point distributions. *Biometrika* 66, 73–79. <https://doi.org/10.1093/biomet/66.1.73>.
- Hoecker, T.J., Higuera, P.E., 2019. Forest succession and climate variability interacted to control fire activity over the last four centuries in an Alaskan boreal landscape. *Landsc. Ecol.* 34, 227–241.
- Hoffman, C., Morgan, P., Mell, W., Parsons, R., Strand, E.K., Cook, S., 2012. Numerical Simulation of Crown Fire Hazard Immediately after Bark Beetle-Caused Mortality in Lodgepole Pine Forests. *For. Sci.* 58, 178–188. <https://doi.org/10.5849/forsci.10-137>.
- Hoffman, C., Sieg, C., Linn, R., Mell, W., Parsons, R., Ziegler, J., Hiers, J., 2018. Advancing the Science of Wildland Fire Dynamics Using Process-Based Models. *Fire* 1, 32. <https://doi.org/10.3390/fire1020032>.
- Hoffman, C.M., Morgan, P., Mell, W., Parsons, R., Strand, E., Cook, S., 2013. Surface Fire Intensity Influences Simulated Crown Fire Behavior in Lodgepole Pine Forests with Recent Mountain Pine Beetle-Caused Tree Mortality. *For. Sci.* 59, 390–399. <https://doi.org/10.5849/forsci.11-114>.
- Johnstone, J.F., Celis, G., Chapin III, F.S., Hollingsworth, T.N., Jean, M., Mack, M.C., 2020. Factors shaping alternate successional trajectories in burned black spruce forests of Alaska. *Ecosphere* 11, e03129. <https://doi.org/10.1002/ecs2.3129>.
- Johnstone, J.F., Chapin, F.S., 2006. Effects of Soil Burn Severity on Post-Fire Tree Recruitment in Boreal Forest. *Ecosystems* 9, 14–31. <https://doi.org/10.1007/s10021-004-0042-x>.
- Johnstone, J.F., Hollingsworth, T.N., Chapin, F.S., Mack, M.C., 2010. Changes in fire regime break the legacy lock on successional trajectories in Alaskan boreal forest. *Glob. Change Biol.* 16, 1281–1295. <https://doi.org/10.1111/j.1365-2486.2009.02051.x>.
- Kelly, R., Chipman, M.L., Higuera, P.E., Stefanova, I., Brubaker, L.B., Hu, F.S., 2013. Recent burning of boreal forests exceeds fire regime limits of the past 10,000 years. *Proc. Natl. Acad. Sci.* 110, 13055–13060. <https://doi.org/10.1073/pnas.1305069110>.
- Lund, M.T., Nordling, K., Gjelsvik, A.B., Samset, B.H., 2023. The influence of variability on fire weather conditions in high latitude regions under present and future global warming. *Environ. Res. Commun.* 5, 065016. <https://doi.org/10.1088/2515-7620/acdfad>.
- Mack, M.C., Walker, X.J., Johnstone, J.F., Alexander, H.D., Melvin, A.M., Jean, M., Miller, S.N., 2021. Carbon loss from boreal forest wildfires offset by increased dominance of deciduous trees. *Science* 372, 280–283.
- McGrattan, K., Hostikka, S., McDermott, R., Floyd, J., Weinschenk, C., Overholt, K., 2024. Fire Dynamics Simulator User's Guide. NIST Spec. Publ.
- McGrattan, K., McDermott, R., Floyd, J., Hostikka, S., Forney, G., Baum, H., 2012. Computational fluid dynamics modelling of fire. *Int. J. Comput. Fluid Dyn.* 26, 349–361. <https://doi.org/10.1080/10618562.2012.659663>.
- Mell, W., 2007. Modeling wildland and wildland-urban interface fires.
- Mell, W., Maranghides, A., McDermott, R., Manzello, S.L., 2009. Numerical simulation and experiments of burning Douglas fir trees. *Combust. Flame* 156, 2023–2041. <https://doi.org/10.1016/j.combustflame.2009.06.015>.
- Mell, W., McNamara, D., Maranghides, A., McDermott, R., Forney, G., Hoffman, C., Ginder, M., 2011. Computer modelling of wildland-urban interface fires 13.

- Mell, W.E., McDermott, R.J., Forney, G.P., Hoffman, C., Ginder, M., 2010. Wildland Fire Behavior Modeling: Perspectives, New Approaches and Applications, p. 17.
- Mueller, E., Mell, W., Simeoni, A., 2014. Large eddy simulation of forest canopy flow for wildland fire modeling. *Can. J. For. Res.* 44, 1534–1544. <https://doi.org/10.1139/cjfr-2014-0184>.
- Overholt, K.J., Kurzawski, A.J., Cabrera, J., Koopersmith, M., Ezekoye, O.A., 2014. Fire behavior and heat fluxes for lab-scale burning of little bluestem grass. *Fire Saf. J.* 67, 70–81. <https://doi.org/10.1016/j.firesaf.2014.05.007>.
- Parks, S.A., Holsinger, L.M., Miller, C., 2015. Wildland fire as a self-regulating mechanism: the role of previous burns and weather in limiting fire progression. *Ecological*.
- Parsons, R., Linn, R., Pimont, F., Hoffman, C., Sauer, J., Winterkamp, J., Sieg, C., Jolly, W., 2017. Numerical investigation of aggregated fuel spatial pattern impacts on fire behavior. *Land Basel* 6, 43.
- Perez-Ramirez, Y., Mell, W.E., Santoni, P.A., Tramoni, J.B., Bosseur, F., 2017. Examination of WFDS in Modeling Spreading Fires in a Furniture Calorimeter. *Fire Technol* 53, 1795–1832. <https://doi.org/10.1007/s10694-017-0657-z>.
- Pimont, F., Dupuy, J.-L., Linn, R.R., Dupont, S., 2011. Impacts of tree canopy structure on wind flows and fire propagation simulated with FIRETEC. *Ann. Forest Sci.* 68, 523. <https://doi.org/10.1007/s13595-011-0061-7>.
- Ritter, S.M., Hoffman, C.M., Battaglia, M.A., Jain, T.B., 2022. Restoration and fuel hazard reduction result in equivalent reductions in crown fire behavior in dry conifer forests. *Ecol. Appl.* 32, e2682. <https://doi.org/10.1002/eap.2682>.
- Ritter, S.M., Hoffman, C.M., Battaglia, M.A., Stevens-Rumann, C.S., Mell, W.E., 2020. Fine-scale fire patterns mediate forest structure in frequent-fire ecosystems. *Ecosphere* 11, e03177.
- Ryan, K., 2002. Dynamic interactions between forest structure and fire behavior in boreal ecosystems. *Silva Fenn* 36. <https://doi.org/10.14214/sf.548>.
- Sánchez-Monroy, X., Mell, W., Torres-Arenas, J., Butler, B.W., 2019. Fire spread upslope: numerical simulation of laboratory experiments. *Fire Saf. J.* 108, 102844. <https://doi.org/10.1016/j.firesaf.2019.102844>.
- Stocks, B.J., Lynham, T.J., Lawson, B.D., Alexander, M.E., Van Wagner, C.E., McAlpine, R.S., Dubé, D.E., 1989. Canadian Forest Fire Danger Rating System: an overview. *Chron* 65, 258–265.
- Turquetly, S., Logan, J.A., Jacob, D.J., Hudman, R.C., Leung, F.Y., Heald, C.L., Yantosca, R.M., Wu, S., Emmons, L.K., Edwards, D.P., Sachse, G.W., 2007. Inventory of boreal fire emissions for North America in 2004: importance of peat burning and pyroconvective injection. *J. Geophys. Res.* 112.
- Veraverbeke, S., Rogers, B.M., Goulden, M.L., Jandt, R.R., Miller, C.E., Wiggins, E.B., Randerson, J.T., 2017. Lightning as a major driver of recent large fire years in North American boreal forests. *Nat. Clim. Change* 7, 529–534. <https://doi.org/10.1038/nclimate3329>.
- Veraverbeke, S., Rogers, B.M., Randerson, J.T., 2015. Daily burned area and carbon emissions from boreal fires in Alaska. *Biogeosciences* 12, 3579–3601. <https://doi.org/10.5194/bg-12-3579-2015>.
- Werth, P., Potter, B., Clements, C., Finney, M., Forthofer, J., McAllister, S., Goodrick, S., Alexander, M., Cruz, M., 2011. Synthesis of Knowledge of Extreme Fire Behavior: volume I for Fire Managers. *JFSP Synth. Rep.*
- Whitman, E., Barber, Q.E., Jain, P., Parks, S.A., Guindon, L., Thompson, D.K., Parisien, M.-A., 2024. A modest increase in fire weather overcomes resistance to fire spread in recently burned boreal forests. *Glob. Change Biol.* 30, e17363. <https://doi.org/10.1111/gcb.17363>.
- Whitman, E., Parisien, M.-A., Thompson, D.K., Flannigan, M.D., 2019. Short-interval wildfire and drought overwhelm boreal forest resilience. *Sci. Rep.* 9, 18796. <https://doi.org/10.1038/s41598-019-55036-7>.
- Ziegler, J.P., Hoffman, C.M., Collins, B.M., Knapp, E.E., Mell, W., 2021. Pyric tree spatial patterning interactions in historical and contemporary mixed conifer forests. California, USA. *Ecol. Evol.* 11, 820–834. <https://doi.org/10.1002/ece3.7084>.
- Ziegler, J.P., Hoffman, C.M., Collins, B.M., Long, J.W., Dagley, C.M., Mell, W., 2020. Simulated Fire Behavior and Fine-Scale Forest Structure Following Conifer Removal in Aspen-Conifer Forests in the Lake Tahoe Basin, USA. *Fire* 3, 51. <https://doi.org/10.3390/fire3030051>.

Further reading

- Kasischke, E.S., Williams, D., Barry, D., 2002. Analysis of the patterns of large fires in the boreal forest region of Alaska. *Int. J. Wildland Fire* 11, 131–144. <https://doi.org/10.1071/wf02023>.
- McGrattan, K., Hostikka, S., 2012. Verification and Validation Process of a Fire Model. *Probabilistic Safety Assessment and Management*. Helsinki.